THE ROYAL SOCIETY PUBLISHING

Electron Microscope Studies of Portland Cement Microstructures during Setting and Hardening [and Discussion]

Author(s): P. L. Pratt, A. Ghose, J. Skalny and P. C. Hewlett

Source: *Philosophical Transactions of the Royal Society of London. Series A, Mathematical and Physical Sciences*, Vol. 310, No. 1511, Technology in the 1990s: Developments in the Science and Technology of Hydraulic Cements (Sep. 24, 1983), pp. 93-103
Published by: The Royal Society
Stable URL: https://www.jstor.org/stable/37467
Accessed: 15-03-2026 17:56 UTC

JSTOR is a not-for-profit service that helps scholars, researchers, and students discover, use, and build upon a wide range of content in a trusted digital archive. We use information technology and tools to increase productivity and facilitate new forms of scholarship. For more information about JSTOR, please contact support@jstor.org.

Your use of the JSTOR archive indicates your acceptance of the Terms & Conditions of Use, available at https://about.jstor.org/terms

The Royal Society is collaborating with JSTOR to digitize, preserve and extend access to *Philosophical Transactions of the Royal Society of London. Series A, Mathematical and Physical Sciences*

This content downloaded from 45.83.136.1 on Sun, 15 Mar 2026 17:56:08 UTC
All use subject to https://about.jstor.org/terms

Phil. Trans. R. Soc. Lond. A **310**, 93–103 (1983) [93]
Printed in Great Britain

Electron microscope studies of Portland cement microstructures during setting and hardening

By P. L. Pratt and A. Ghose†
Department of Metallurgy and Materials Science, Imperial College, Prince Consort Road, London SW7 2BP, U.K.

[Plates 1 and 2]

The rates of hydration of the individual phases in Portland cement have been related both to the disappearance of these phases from the microstructure and to the appearance of their products of hydration.

After 12–15 h hydration a shell of product is formed containing short rods of AFt, an infilling of C–S–H and ettringite rods 1–2 μm long from the hydration of C_3A. Later hydration takes the form of Hadley grains, by dissolution of the core from inside the shell and precipitation of product either inside the shell or in between the shells. The network of shells forms the cohesive element in the system after 10–12 h, with the coherent inner product filling up the space progressively inside the shells but not being attached to them. The implication of these loose fillings for the tensile strength and permeability are discussed.

The onset of rapid hydration of C_4AF has been identified by quantitative X-ray diffraction with a new peak found by conduction calorimetry; in the microstructure, fibres of AFt phase, 5 μm or more in length, appear suddenly from the C_4AF and these are a familiar feature of O.P.C. pastes after 2 or 3 days hydration. After about 5 days at 20 °C the local availability of water is reduced and the rate of hydration of all the phases is reduced.

1. Introduction

In previous papers on C_3S (Jennings *et al.* 1981) and on Portland cement (Dalgleish *et al.* 1982*a*), electron microscope techniques were combined with a variety of methods of specimen preparation to examine the development of the microstructure with time of hydration. Differences between early, middle and late products of hydration were identified and these differences were related to the stages of hydration by using an isothermal calorimeter. Despite early suggestions that the various clinker compounds in normal Portland cements have the same partial rate of hydration (Brunauer 1957), subsequent work has shown that this is not the case. Locher (1981) showed clearly that the induction period for C_3S in Portland cement ends well before that for C_3A and this is confirmed by the X-ray data of Osbaeck & Jons (1980). In this paper the rates of hydration of the individual phases in Portland cement are related both to the disappearance of those phases from the microstructure and to the appearance of the products of their hydration. Thereby new features of the mechanisms of hydration of cement are revealed. Since the earliest stages of hydration have received attention recently (Dalgleish *et al.* 1981; Dalgleish *et al.* 1982*b*), this paper will concentrate on hydration from 24 h and onwards.

† Present address: Department of Civil Engineering, University of Illinois at Urbana-Champaign, Urbana, Illinois 61801, U.S.A.

This content downloaded from 45.83.136.1 on Sun, 15 Mar 2026 17:56:08 UTC
All use subject to https://about.jstor.org/terms

2. Experimental methods

The reactions occurring in the cement pastes and the resulting development of microstructure were studied with conduction calorimetry, quantitative X-ray diffractometry, and scanning electron microscopy. Northfleet o.p.c. was mixed with distilled water at a water/cement ratio of 0.5. For calorimetric studies, a Wexham Instruments isothermal calorimeter was used at 20 °C. The specimens were mixed by kneading for 5 min in a polythene bag outside the calorimeter so that the first heat peak was missed. For s.e.m. observations, the pastes were cast into small cylindrical moulds, sealed and left to cure at room temperature. At appropriate times the moulds were split open, the specimens fractured in bending while still wet and immediately flooded with isopropanol to stop the hydration reactions. After about 15 min, they were dried in an oven for about 2 h, mounted on stubs, coated with 25–30 nm of gold and stored in a vacuum desiccator until the s.e.m. was available. For q.X.r.d., part of the s.e.m. specimen was powdered in a micronizing mill and measurements and analysis were done at the Cement and Concrete Association, Wexham Springs.

Table 1. Cement composition (%)

chemical		Bogue		q.X.r.d.	
SiO_2	20.3	C_3S	59.0	C_3S	67.0
Al_2O_3	5.2	C_2S	13.7	β-C_2S	13.0
Fe_2O_3	3.1			α-C_2S	2.0
CaO (total)	64.7	C_3A	8.5	C_3A	5.0
Na_2O	0.19	C_4AF	9.4	C_4AF	6.0
MgO	1.1	$\bar{\bar{K}}$ (total)	0.63	anhydrite	2.0
K_2O	0.34			hemihydrate	2.5
SO_3	2.8				
free lime	0.7				

The composition of the Northfleet cement is given in table 1. The difference between the Bogue analysis and that measured by q.X.r.d. is significant especially for the aluminate phases. The specific surface area was 341 $m^2\ kg^{-1}$. This standard production Northfleet o.p.c. is similar to that used before (Dalgleish *et al.* 1981; Dalgleish *et al.* 1982*a*) and is the same as cement B in the paper by Dalgleish *et al.* (1982*b*). (In the latter publication the Bogue composition for cement B is reported incorrectly although the oxide analysis is correct.) Particle size analysis of the Northfleet o.p.c. with a Coulter counter showed up to 30 % (by volume) of particles greater than 30 μm and up to 3 % greater than 90 μm. Many of the large particles were polymineralic, but the average particle size for those that were largely C_3S, or alite, was 20–25 μm.

3. Experimental results

(*a*) *Degree of hydration of cement phases*

The rate of heat evolution with time for the Northfleet o.p.c. is shown in figure 1. As we have noticed previously with this cement (Ghose & Pratt 1981), in addition to peak 2, which is due to the hydration of C_3S forming middle product C–S–H/CH, and peak 3, which is due to the hydration of C_3A forming rods of ettringite, a distinct peak 4 can be seen. This peak is accelerated and enhanced by the replacement of 30 % of the o.p.c. by fly ash. This peak 4 has now been identified by q.X.r.d. as marking the onset of rapid hydration of C_4AF. During peak 4,

This content downloaded from 45.83.136.1 on Sun, 15 Mar 2026 17:56:08 UTC
All use subject to https://about.jstor.org/terms

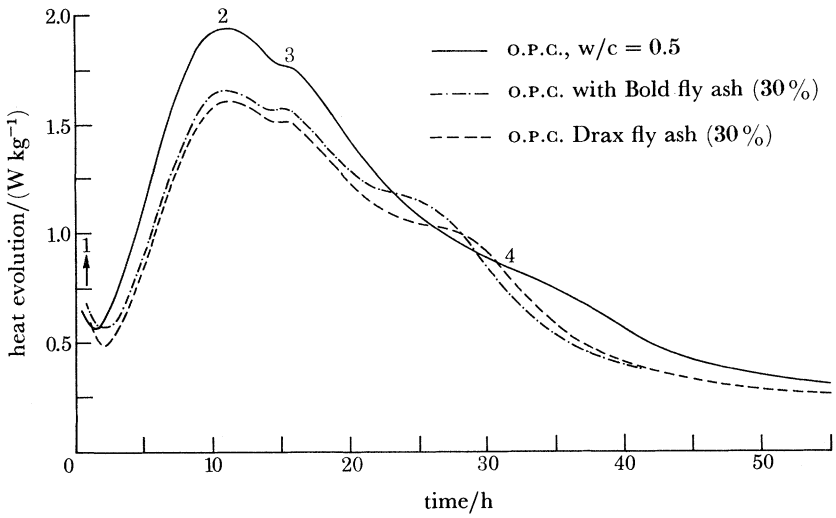

FIGURE 1. The rate of evolution of heat at 20 °C for Northfleet o.p.c. and o.p.c. with fly ash blends at w/s ratio 0.5.

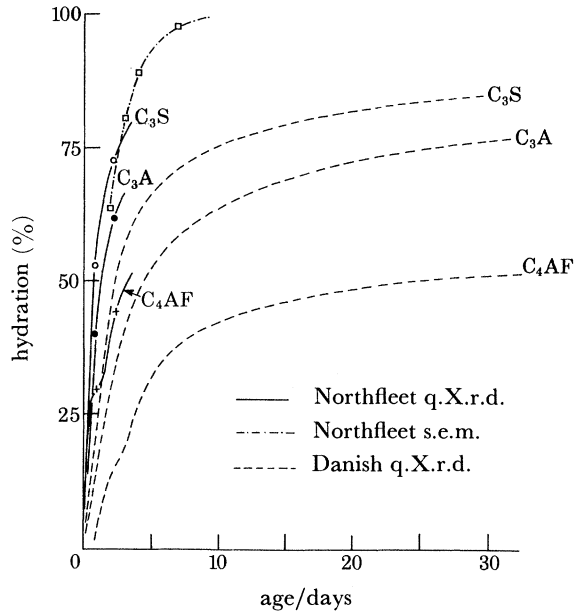

FIGURE 2. The degree of hydration as a function of time for the individual phases in Northfleet cement. Data for Danish cement at w/c ratio 0.44, after Jons & Osbaeck (1982).

hydration of some 10 % of the C_4AF in neat cement paste takes place, and 20 % in the cement/fly ash mixtures. Fukuhara *et al.* (1981) have measured the heat of hydration for C_4AF and gypsum to form AFt as 724 J/g. From this figure, with the percentage of C_4AF that hydrated during peak 4 determined by q.X.r.d., the total heat evolved during peak 4 can be accounted for satisfactorily (Halse & Pratt 1983).

The recent X-ray data of Osbaeck & Jons (1980) and Jons & Osbaeck (1982) on the hydration of cement phases is more complete than ours and part of their data is plotted together with ours in figure 2. In both cements the rates of hydration of the phases C_3S, C_3A and C_4AF differ

This content downloaded from 45.83.136.1 on Sun, 15 Mar 2026 17:56:08 UTC
All use subject to https://about.jstor.org/terms

significantly; C_3S hydrates faster than C_3A, whereas C_4AF lags noticeably behind. The data for C_2S are less reliable but by 28 days some 25 % has hydrated. The Danish cement resembles the Northfleet O.P.C. with a $\bar{\bar{K}}$ (total) of 0.75 % compared with our 0.63 %, although by Bogue analysis it contains 51 % C_3S and 27 % C_2S, compared with our 59 % and 13.7 % by Bogue.

(*b*) *Development of microstructure*

As with all the cements we have examined (Dalgleish *et al.* 1982*a*, *b*), the early formation of very short rods of AFt, 0.2 μm long, on the surface of the particles is followed at the end of the induction period for C_3S by the build-up of a thickening shell of C–S–H around the cement grains engulfing the AFt. After 12 h hydration this shell is between 0.5 and 1 μm thick and the cohesion between neighbouring shells is strong enough to enable the paste to be broken into two pieces without collapsing to powder. The fracture path runs through the shell in many places, revealing the formation of Hadley grains with a hollow space between the shell and the hydrating core. Longer rods of ettringite appear at about this time (10–12 h) associated with the end of the induction period for C_3A, peak 3 in figure 1. Some of these are clustered in the form of small spherulites but most appear as outgrowths from the shell of the Hadley grains with a length of 1–2 μm.

After 24 h hydration, the Northfleet O.P.C. shows many Hadley grains, figure 3, plate 1, with the characteristic spiky shell of ettringite rods and type I C–S–H. Most of the top of this micrograph shows the inner surface of a Hadley shell some 25 μm across with remnants of the hydrating core, which has been pulled away. In this micrograph there are a further nine Hadley grains, which can be seen by the practised eye; some like that in the centre of the figure have a lamellar core, which is believed to be from C_3A, and others like that at the top of the figure come from C_3S. Large crystals of CH grow up to 50 μm in size in the original water space and in this form they can be seen even after 4–5 days where the fracture path is inter-granular.

After 2 days, the induction period for C_4AF has ended, leading to peak 4, and a new and coarser morphology of AFt fibres appears, figure 4, typically 5 μm in length or more. This sudden appearance is even more noticeable with fly ash added to the cement, as would be expected from figure 1. The earlier rods of ettringite from the C_3A, 1–2 μm in length, are still visible in the background and the new long fibres of AFt are recognized as a familiar feature of s.e.m. micrographs of O.P.C. pastes after 2 or 3 days hydration. X-ray analysis shows that these fibres contain significant quantities of Al, $\bar{S}$ and Fe as well as Ca. In some Hadley grains the core appears to have contained both C_3A and C_4AF, from which the Ca, the Al, and only part of the Fe has dissolved, leaving amorphous iron-rich regions (Fukuhara *et al.* 1980). At this age the shells are starting to thicken by deposition of C–S–H and CH inwards. In figure 4 this thickening of the shell can be seen around a polymineralic Hadley grain. The upper part of the grain, largely dissolved, resembles that associated with C_3A in figure 3, whereas the lower

---

Description of plate 1

Figure 3. 1 day hydration. Hadley grains, with ettringite rods.

Figure 4. 2 days hydration. Hadley grains with coarse AFt fibres.

Figure 5. 3 days hydration. C_3S core.

Figure 6. 4 days hydration. C_3S core.

Figure 7. 4 days hydration. α'-C_2S core.

Figure 8. 4 days hydration. β-C_2S emerging in C_3S core.

This content downloaded from 45.83.136.1 on Sun, 15 Mar 2026 17:56:08 UTC
All use subject to https://about.jstor.org/terms

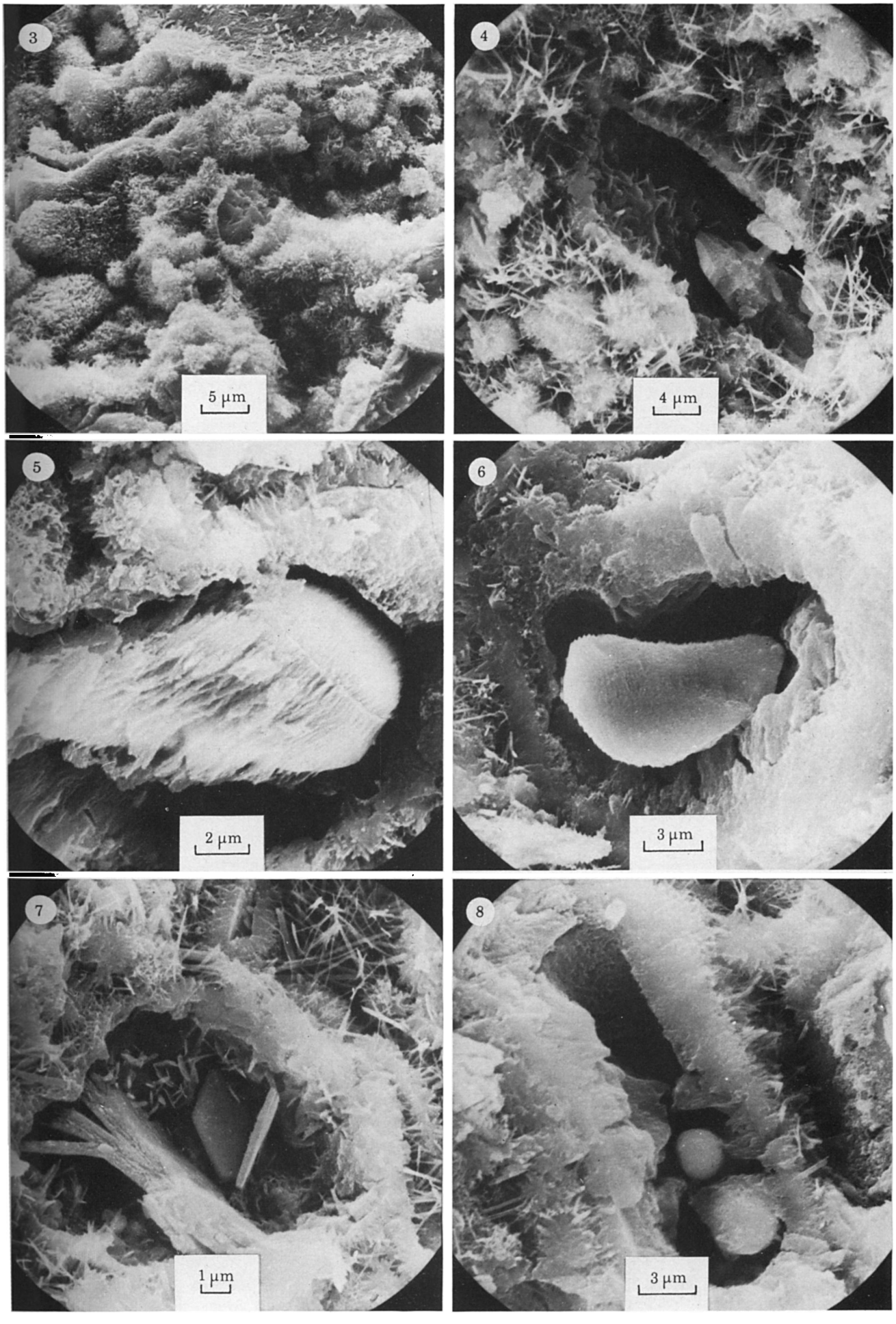

Figures 3–8. For description see opposite.

(*Facing p.* 96)

This content downloaded from 45.83.136.1 on Sun, 15 Mar 2026 17:56:08 UTC
All use subject to https://about.jstor.org/terms

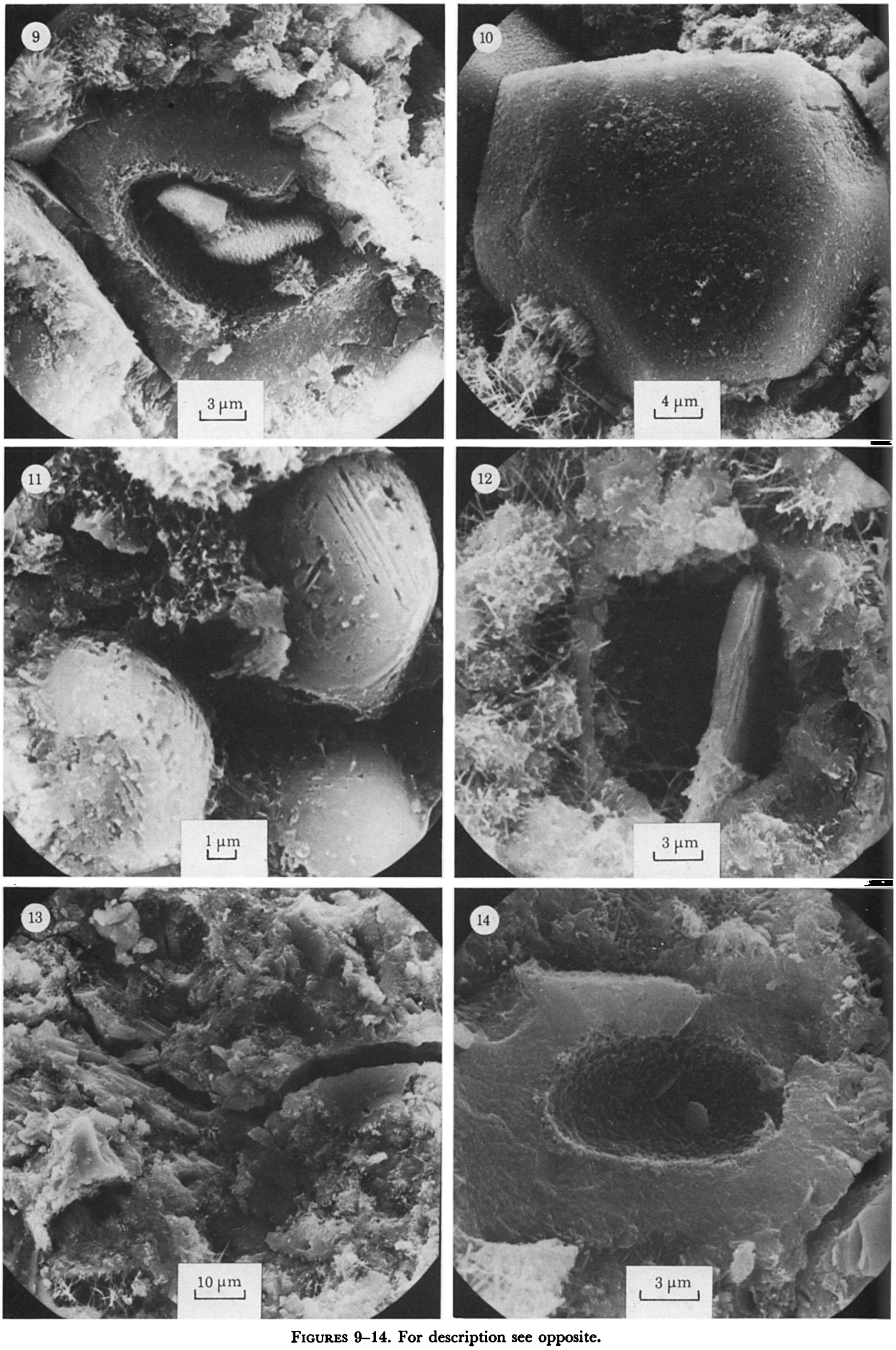

Figures 9–14. For description see opposite.

This content downloaded from 45.83.136.1 on Sun, 15 Mar 2026 17:56:08 UTC
All use subject to https://about.jstor.org/terms

has the serrated appearance of the C_3S core in figure 5. After 3 days the shells have thickened to 2–3 μm, the C_3S cores are dissolved away substantially, figure 5, sometimes revealing spheres of β-C_2S, while the occasional large particle of C_4AF has continued to dissolve. At this time squat hexagonal platelets can be seen inside some of the shells although their occurrence is rare. They are believed to be the α′-C_2S, which makes up 2 % of this O.P.C. By this time the inward growth of the C–S–H/CH into the centre of the Hadley grain is becoming more noticeable and after 4 days, especially around C_3S cores, figure 6, the shell thickness can approach 5 μm. The smaller C_3S Hadley grains are by now almost filled with flaky C–S–H/CH whereas those that contain α′-C_2S cores, figure 7, remain relatively empty. Inside this particular shell, plates of AFm are growing inwards together with larger plates of CH. Outside the shell, however, both fine rods of ettringite and coarse fibres of AFt remain stable, suggesting that the shortage of gypsum is confined to the region within the shell. The C–S–H outside the shell appears to have dried into a type II morphology and this is fairly typical of the outer C–S–H at 4 days in this cement. The inner C–S–H/CH, especially in figure 8, has a characteristically porous appearance, composed of flakes or flattened equant grains growing together. Inside this shell, small rounded particles of β-C_2S are emerging from the dissolving C_3S.

After 7 days, the C_3S cores revealed by fracture continue to dissolve and the inner products continue to fill up the empty space within the shell around them, figure 9, plate 2. Depending upon the original particle size, the thickness of the shell can exceed 10 μm, so that particles originally 20 μm across could be filled with inner product. Depending upon the fracture path, the inner product can appear to take up the morphology of the original particle in the O.P.C., figure 10, in this case an angular alite grain overlying its neighbour. The mottled inner product is now coherent in itself but, in the dried state, it is detached from the outer Hadley shell save for a few patches of contact. In Hadley grains containing C_3S and β-C_2S, the β-C_2S starts to etch after 7 days, although the access of water is limited by the coherence of the inner product surrounding it. Between the Hadley grains the intergrowths of massive CH crystals are filling up the structure, although long fibres of AFt and spherulites can still be seen. The crack path has become flatter, with a substantial proportion of intra- rather than inter-granular fracture, and stepped cleavage planes through the massive CH crystals become a prominent feature. After 14 days this transparticle fracture becomes even more noticeable and at the same time the dissolution of C_2S, figure 11, is well under way.

After 28 days, some hollow shells remain, particularly those containing α′-C_2S, figure 12, and β-C_2S, both of which have hydrated now by some 25 %. After 2 months, the overall porosity is reduced and transparticle fracture is predominant, with large areas of cleavage through CH, figure 13. Outlines of former Hadley grains can be recognized by the structure of the outer shell and the fibres of AFt remaining in the unfilled interstices. Coherent inner product can be recognized on the fracture surface, figure 14, within which all the C_3S has

Description of plate 2

Figure 9. 7 days hydration. C_3S core and mottled inner product.

Figure 10. 7 days hydration. Inner product detached from shell.

Figure 11. 14 days hydration. β-C_2S in core.

Figure 12. 1 month hydration. α′-C_2S in core.

Figure 13. 2 months hydration. Transparticle fracture.

Figure 14. 2 months hydration. Detached inner product.

This content downloaded from 45.83.136.1 on Sun, 15 Mar 2026 17:56:08 UTC
All use subject to https://about.jstor.org/terms

hydrated, leaving rounded cavities with a few small platelets of CH; this inner product has cracked away from the original outer shell. In other areas of figure 13, long rods of AFt can still be seen and these appear to be a permanent feature of the microstructure, at least up to 8 months. Between 2 and 4 months some of the rounded cavities in the coherent inner product fill slowly with a different form of C–S–H presumably coming from the hydration of C_2S.

4. Discussion

(*a*) *Rates of hydration of cement phases*

(i) C_4AF

The addition of 30 % fly ash accelerated and enhanced peak 4 in the calorimeter curve in figure 1 and, for these blended pastes also, q.X.r.d. confirmed that the peak was due to the onset of rapid hydration of C_4AF. The pozzolanic reaction with CH is known to start in this blend after some 24 h hydration (Halse & Pratt 1983) and this provides the clue to understanding the enhancement of peak 4. Fukuhara *et al.* (1980) measured the rate of heat evolution for the hydration of C_4AF with additions of gypsum and lime, showing that the more lime was added the more the main hydration peak was retarded. The pozzolanic reaction of the fly ash reduces the quantity of CH in the hydrating system by forming C–S–H and consequently both accelerates and enhances the hydration of C_4AF. Similar effects would be expected with slag cements and with the addition of silica fume; a large early peak 4 can be seen in both (Goult & Pratt 1983). This same explanation can account for the different rates of hydration of C_4AF in cements of different alkali content (Osbaeck & Jons 1980). Increased alkali content accelerates the hydration of C_3S in the first few days, thereby increasing the quantity of CH in the system. The retarding effect on the hydration of C_4AF is very obvious from their data and it would be interesting to confirm this hypothesis by microscopic observation.

(ii) C_3S *and* C_3A

Whereas Mindess & Young (1981) in their recent textbook suggest that the hydration of C_3A in Portland cement paste is faster than that of C_3S, the data in figure 2 show that this is not so, at least for the Danish and British cements. Locher (1981) showed that for German Portland cement the induction period for C_3S ends well before that for C_3A so long as the cement contains gypsum, while the hydration of C_3S is the faster of the two. This agrees with our interpretation of peak 3 as the onset of hydration of C_3A giving rods of ettringite 1–2 μm in length, outside the Hadley shells. Fine particles of C_3A, and also of C_4AF, react during the first few minutes in peak 1 to form the amorphous gel layer with short rods of AFt 0.2 μm in length, seen in the microscope, but thereafter C_3S starts earlier and is the faster to hydrate in all three European cements. It would be interesting to know why the American cement referred to by Mindess & Young appears to behave differently.

(iii) C_3S, C_3A *and* C_4AF

Taplin (1959) measured the effect of w/c ratio upon the overall rate of hydration, assuming that all the cement phases hydrate at the same rate. He found a marked decrease in rate, at increasing degrees of hydration with increasing w/c, and this he ascribed to the filling up of available water space with hydration products. While allowances have to be made for the distribution of the sizes of the hydrating particles (Taplin 1969), at first sight the rates of

This content downloaded from 45.83.136.1 on Sun, 15 Mar 2026 17:56:08 UTC
All use subject to https://about.jstor.org/terms

hydration of C_3S, C_3A and C_4AF in the Danish cement in figure 2 all decrease markedly after about 5 days, the aluminate phases more sharply than C_3S. Rather than suggesting the filling of space with hydration product, this decrease in hydration rate suggests that the local availability of water to the anhydrous phases becomes reduced at this time.

(*b*) *Degree of hydration and development of microstructure*

The degree of hydration of the various phases measured by q.X.r.d. in figure 2 represents the average degree of hydration for the paste as a whole. At a particular time the smallest particles of one phase may be fully hydrated while the largest will remain largely unhydrated. Only the mean particle size will approximate to the rate of hydration shown in figure 2. For C_3S, or better alite, particles, figures 5, 6, 9 and 14 represent the sequence of hydration from 2 days to 2 months for particles originally about 20 μm in diameter. The volume of the alite cores remaining can be estimated crudely from these micrographs and these particles appear to be hydrating faster than the Danish cement, in agreement with our X-ray data in figure 2.

For C_3A the picture is less clear because identification of the C_3A particles is less obvious. The lamellar regions seen inside the Hadley shells in figures 3, 4 and 8 could be remnant C_3A, or alternatively they could be plates of monosulphate or hexagonal C_4AH_{13} where the SO_4^{2-} ion had difficulty in penetrating. Further work is needed to confirm the identity and the rate of hydration of these phases.

The work of Fukuhara *et al.* (1980) on the hydration of C_4AF makes it clear that the fibrous product AFt contains much less iron than the C_4AF from which it came. They suggested that an amorphous relict phase, rich in iron, with the same shape as the original C_4AF particle was left after dissolution of the material needed to form the AFt. Striated regions within the shell are a common feature of Hadley grains in cement after 2 days and their appearance coincides with that of the long coarse AFt fibres containing iron.

The hydration of α'-C_2S is somewhat faster than that of β-C_2S (Jelenić-Bezjak 1983) and the squat hexagonal platelets in figures 7 and 12 are believed to represent this phase. Some dissolution has occurred by 4 days but the rate of hydration is slow. Unlike the C_3S, these Hadley shells appear to remain largely unfilled as late as 1 month, when perhaps 25–30 % of the phase should have hydrated. By contrast, β-C_2S starts dissolving after 7 days but is frequently found inside Hadley grains in which C–S–H from the adjacent C_3S, figure 11, has already surrounded it. Under these circumstances, unlike α'-C_2S, the hydration is starting only when the free access of water has already been reduced, so that the rate is bound to be slow.

(*c*) *Mechanisms of hydration*

This microstructural study suggests that the presence of the interstitial aluminate phases in Portland cement determines the mechanisms of hydration. The principal difference between the hydration of O.P.C. and that of pure C_3S is the early formation of a shell around the cement grains in the former and the subsequent dissolution of the core from within this shell. The network of shells forms the coherent element in the hydrating cement system after 10–12 h and the space left both between the shells and within the shells is filled progressively by a variety of products.

(i) *Formation of the shell*

The skeleton of the hydration shell appears to be the short rods of AFt formed during peak 1

This content downloaded from 45.83.136.1 on Sun, 15 Mar 2026 17:56:08 UTC
All use subject to https://about.jstor.org/terms

from the dissolution of C_3A and C_4AF. The infilling of this skeleton with C–S–H and some CH starts at the end of the induction period for C_3S and is almost completed by the top of peak 3 when the first Hadley grains were found. At the same time, renewed hydration of C_3A gives rise to rods of ettringite, 1–2 μm in length, bursting out from the shells and leaving empty space behind them. Recent experiments by Goult & Pratt (1983) show that hollow shells can form during the hydration of cements containing C_4AF and only very little C_3A. By q.X.r.d., Jons & Osbaeck (1982) found no ettringite after 1 day in a similar cement that contained 18 % C_4AF and no C_3A. After 3 days, ettringite, or more probably AFt, was present and no conversion to monosulphate was found by 28 days.

(ii) *Filling of space between the shells*

A major contribution to the filling of the original water space between cement particles after 12 h comes from the large crystals of CH. The corresponding C–S–H appears to be retained largely in the shell as infilling. The onset of hydration of C_3A covering the outer surface of the shells with ettringite rods, 1–2 μm long, figure 3, makes a further significant contribution, at the expense of creating space inside the shells. The onset of hydration of C_4AF after about 30 h gives rise to long coarse fibres of AFt, many of which are associated with spherulites (Dalgleish *et al.* 1982). These arise from the large number of small particles of the interstitial phase of the cement that contain C_4AF. The formation of monosulphate starts inside the shells as early as 24 h, where the supply of gypsum is limited. For their Danish cement, Jons & Osbaeck (1982) have shown that equal amounts of ettringite and monosulphate are present after 3 days, some of the monosulphate having formed by conversion of the ettringite. Although some ettringite rods and AFt fibres remain in open pores as late as 8 months, many must be converted to monosulphate as the hydration products continue to fill the original water space between the particles. The release of water as this conversion takes place enables the hydration to continue, although this water is released outside the original Hadley shells rather than inside, where the bulk of the unhydrated material remains.

(iii) *Filling of space within the shells*

Part of the difficulty of accepting the formation of Hadley grains as the principal mechanism of hydration from the top of peak 2 onwards has been the problem of the density of hydrated cement paste, if it is indeed full of hollow shells. The filling of shells containing C_3S, i.e. the majority of the shells in the cement, can now be seen to take place by dissolution of the core and precipitation of an intimate mixture of C–S–H/CH on the inside of the shell, figures 6, 9, 10 and 14. This inner product takes up the form of the original particle, figure 10, and protects the core, effectively cutting it off from the original water space after 5–6 days. This intimate mixture of product should have a C/S ratio reflecting the composition of the material within the core, approaching 3 if the core was largely C_3S and all the products were retained within the shell; Diamond (1976) has found a C/S ratio 2.96 for this inner product. It forms the greater part of the products of hydration of cement paste and can be recognized easily on the fracture surface of mature pastes. Often there is sufficient C_3S inside the shell to fill it with this product, but sometimes, as in figure 14, there is not. These cavities may be filled subsequently with product of a different texture coming either from the larger C_3S grains or from C_2S.

This content downloaded from 45.83.136.1 on Sun, 15 Mar 2026 17:56:08 UTC
All use subject to https://about.jstor.org/terms

(iv) *Types of* C–S–H *in hydrated* O.P.C.

On the dried s.e.m. specimens, rolled-up foils and fibres of type I C–S–H (Diamond 1976), which start to form during the first few hours, remain visible for 3–4 days on the outer surfaces of the Hadley grains. Further hydration of C_3S leads to infilling at the roots of the fibres with the appearance of reticular type II C–S–H after 3 days. These are both artefacts of drying, reflecting the way in which the wet outer layers of C–S–H shrink and thus reduce their surface area. Diamond (1976) has designated the inner product morphology as type IV C–S–H, identifying it by its dimpled appearance with either regular pores or close packed equant grains about 0.1 μm in size. He suggested that recognizable 'inner product' will be lacking to the extent that the cement dissolves from within the Hadley shell. We have seen that dissolution of C_3S is followed by precipitation of C–S–H/CH within the shell. To this extent we believe that type IV C–S–H is the most common product in our cements. Type III C–S–H is more difficult to identify; some of Diamond's micrographs appear to refer to infilling in the Hadley shell, some to the core of spherulites and some to the products of hydration of small particles of alite.

(*d*) *Implications for strength and durability*

A number of implications for the strength, durability and permeability of hardened cement pastes arise from these observations of the microstructure and the modes of hydration. Perhaps the most important relates to the way in which the coherent type IV C–S–H/CH structure develops inside the original Hadley shell. In figure 10, at 7 days, and in figure 14, after 2 months, this structure in the dried state is detached from the outer Hadley shell save for a few isolated patches of contact. While the compressive strength of this microstructure may be high, the tensile strength and thus the modulus of rupture will be low. This strength will be related to the tensile strength of the original network of interconnected shells, with the maximum particle size, of more than 100 μm, determining the size of the largest inherent Griffith flaw. Extraneous defects in the form of the trapped air bubbles found in hand-mixed cement pastes can be removed by vacuum treatment of the fresh paste shortly after mixing. As we would expect, de-aired cement paste shows no substantial improvement in mechanical properties in the hardened state because this treatment does not alter the mechanism of hydration of the cement.

5. Conclusions

1. Rapid hydration of C_4AF in O.P.C. starts after 2–3 days and *ca.* 40 % has hydrated by the end of peak 4. Removal of CH by pozzolanic reaction accelerates and accentuates this hydration.

2. C_3S hydrates earlier and faster than most of the C_3A in O.P.C.

3. After 5 days at 20 °C and w/c 0.5, the hydration of C_3S, C_3A and C_4AF slows down, owing to the restricted access of water to the unhydrated phases.

4. C_3S, α'-C_2S, β-C_2S, C_3A and C_4AF together with their hydration products can be identified in the microstructure during the course of hydration.

5. The formation of a hydration shell after 12 h is followed by progressive dissolution of C_3S, C_4AF, and C_2S. The network of shells forms the coherent element in hydrating O.P.C. pastes and is responsible for many of their late properties.

6. The space between the shells is filled with large intergrowths of CH, ettringite rods from C_3A, AFt fibres and spherulites from C_4AF, and C–S–H from C_2S and large-grained C_3S.

This content downloaded from 45.83.136.1 on Sun, 15 Mar 2026 17:56:08 UTC
All use subject to https://about.jstor.org/terms

7. The space within the shells is filled with inner product largely from within.

8. This inner product is detached from the shell and may consequently form an inherent Griffith flaw in hardened cement paste.

The authors wish to thank the Marine Technology Directorate of S.E.R.C. for financial support of this work, Blue Circle for the provision of cement, Mr Gutteridge for doing the quantitative X-ray diffraction analysis and identifying peak 4, figure 1, at the Cement & Concrete Association, Wexham Springs, and their colleagues for helpful discussions. In particular, they thank Karen Scrivener for commenting on the draft of the paper and Grace Halse for providing figure 1.

References

Brunauer, S. 1957 In *The science of engineering materials* (ed. J. E. Goldman), pp. 460–466. New York: Wiley.

Dalgleish, B. J., Ghose, A., Jennings, H. M. & Pratt, P. L. 1981 In *Proc. 11th Int. Conf. Sci. Ceram., Sweden*, vol. 2 (ed. R. Carlsson & S. Karlsson), pp. 297–302. Gottenburg: Swedish Ceramic Society.

Dalgleish, B. J., Ghose, A., Jennings, H. M. & Pratt, P. L. 1982*b* In *Int. Conf. Concr. at Early Ages, Paris*, vol. 1, pp. 137–143.

Dalgleish, B. J., Pratt, P. L. & Moss, R. I. 1980 *Cem. Concr. Res.* **10**, 665–676.

Dalgleish, B. J., Pratt, P. L. & Toulson, E. 1982*a* *J. Mater. Sci.* **17**, 2199–2207.

Diamond, S. 1976 In *Proc. Conf. Hydraulic Cement Pastes; their Structure and Properties, Sheffield*, pp. 2–30. Wexham Springs: Cement and Concrete Association.

Fukuhara, M., Goto, S., Asaga, K., Daimon, M. & Kondo, R. 1981 *Cem. Concr. Res.* **11**, 407–414.

Fukuhara, M., Goto, S., Asaga, K., Daimon, M., Kondo, R. & Ono, Y. 1980 *J. ceram. Soc. Japan* **88** (8), 436–440.

Ghose, A. & Pratt, P. L. 1981 In *Proc. Symp. Effects of Fly ash Incorporation in Cement & Concrete*, pp. 82–91. Boston: Materials Research Society.

Goult, D. J. & Pratt, P. L. 1983 To be presented at 1st Int. Conf. on Use of Fly ash, Silica Fume, Slag and Other Mineral By-Products in Concrete, Montebello.

Halse, Y. H. & Pratt, P. L. 1983 To be presented at 1st Int. Conf. on Use of Fly ash, Silica Fume, Slag and Other Mineral By-Products in Concrete, Montebello.

Jelenić-Bezjak, I. 1983 In *Advances in cement technology* (ed. S. N. Ghosh), pp. 397–440. Oxford: Pergamon Press.

Jennings, H. M., Dalgleish, B. J. & Pratt, P. L. 1981 *J. Am. ceram. Soc.* **64** (10), 567–572.

Jons, E. S. & Osbaeck, B. 1982 *Cem. Concr. Res.* **12**, 167–178.

Locher, F. W. 1981 In *Proc. 7th Int. Congr. Chem. Cem., Paris*, vol. IV, pp. II. 49–II. 62. Paris: Éditions Septima.

Mindess, S. & Young, J. F. 1981 In *Concrete* (ed. N. M. Newmark & W. J. Hall), New Jersey: Prentice-Hall.

Osbaeck, B. & Jons, E. S. 1980 In *Proc. 7th Int. Symp. Congr. Cem., Paris*, vol. II, pp. II. 135–II. 140. Paris: Éditions Septima.

Taplin, J. H. 1959 *Aust. J. appl. Sci.* **10**, 329–345.

Taplin, J. H. 1969 In *Proc. 5th Int. Symp. Chem. Cem., Tokyo*, vol. II, p. 249.

Discussion

J. Skalny (*Martin Marietta, Baltimore, U.S.A.*). What are the reasons for the absence of Hadley grains in pure C_3S hydration? What is the mechanistic explanation?

P. L. Pratt. In the cements we have examined, the presence of Hadley grains is associated with the formation of a network of shells around the cement particles arising from the interstitial aluminate phases. The first skeleton of this shell comes from the very early hydration of C_3A and C_4AF forming short rods of AFt within or on an amorphous gel coating. This skeleton is built on during peak 2, with middle product C–S–H from C_3S and from exposed small particles of C_2S. Finally, the hollow shells appear rapidly as C_3A hydrates during peak 3, and form rods of ettringite outside the shells, leaving space within. In pure C_3S, the absence of the aluminate phases prevents the early formation of the skeleton and also its subsequent growth. In C_3S the formation of a rim of C–S–H does slow down the hydration in the later stages, but

This content downloaded from 45.83.136.1 on Sun, 15 Mar 2026 17:56:08 UTC
All use subject to https://about.jstor.org/terms

this rim of product seems to be more flexible than the shell in O.P.C. Occasionally, hollow shells have been seen in alites and in some large particles of C_3S, but only after 14–28 days rather than 12–24 h.

P. C. HEWLETT (*Cementation Research Ltd., Rickmansworth, U.K.*). Professor Pratt implied that the tensile strength of hydrated Portland cement was in some way associated with the gap between the 'outer' and 'inner' hydration layers. What is the cause of the gap and what can be done to overcome it to upgrade tensile strength?

P. L. PRATT. The cause of the gap between the outer and inner hydration layers appears to be the different mechanisms of hydration responsible for the two products. Initially, the hollow space inside the shell is associated with the onset of the rapid hydration of C_3A, to form ettringite rods, 1–2 μm long, outside the shell. The inner surface of the shell then consists of some areas of AFm, where the supply of sulphate ions is limited, and some of the less soluble remains of the cement grains. Occasionally these inner surfaces form a good basis for the nucleation and growth of the inner product inwards but most of the inner product appears to be a loose fit within the shell. Differential shrinkage and later dissolution and hydration of the less soluble remains could play a part in this separation.

If indeed this gap is associated with the low tensile strength of hydrated Portland cement, some way of overcoming it should be found. Recognized ways of increasing the strength include warm pressing the products together in an autoclave, modifying the mechanism of hydration by high shear mixing so as to break down the early AFt shells, or minimizing the amount of hydration, so that hollow shells do not form, with a polymer additive to lubricate and glue the particles together. A less drastic way would be to study the bond between the inner and outer products and, by adjusting the chemistry and mechanisms of the reactions, maximize the strength of the bond.

This content downloaded from 45.83.136.1 on Sun, 15 Mar 2026 17:56:08 UTC
All use subject to https://about.jstor.org/terms